Modeling Jupiter's Synchrotron Radiation

Steven M. Levin, Scott J. Bolton, Bidushi Bhattacharya, Samuel Gulkis and Michael J. Klein

Jet Propulsion Laboratory, California Institute of Technology, Pasadena, California

Richard M. Thorne

Department of Atmospheric Sciences, UCLA, Los Angeles, California

Abstract.

We have constructed a computer model to simulate the synchrotron emission from relativistic electrons trapped in Jupiter's magnetic field. Our computer program generates the four Stokes parameters of the synchrotron emission for assumed electron distributions and magnetic field models. The resulting two dimensional Stokes parameter maps can be compared directly with ground based observations. We use magnetic field models derived from spacecraft measurements, and tailor the electron distributions to fit synchrotron observations. The gross features of data from both VLA and single-dish observations are fit by a longitudinally symmetric particle distribution. We suggest that higher order terms in the magnetic field are primarily responsible for the observed rotational asymmetry.

Introduction

Synchrotron radio emission from Jupiter, observed from the Earth, provides an important tool for understanding the magnetic field and relativistic electron population in the inner (1.2 to 3.5 Jovian radii) Jovian magnetosphere. Measurements of the synchrotron emission dating back to the late 1950's were used to infer the presence of a magnetic field on Jupiter, its polarity and dominant dipole structure, the orientation of its dipole axis relative to Jupiter's rotational axis, and the presence of relativistic electrons in the inner magnetosphere. Very high resolution radio maps of the synchrotron emission made with the VLA and other arrays have provided a wealth of additional information on the emission [e.g., *dePater* et al. 1997, *LeBlanc* et al. 1997 and references therein]. Measurements from *in situ* spacecraft (Pioneers and Voyagers) and observations of Io's footprint [*Connerney* et al. 1998] have greatly improved our knowledge of the magnetic field, especially our knowledge of the higher order moments. To date, it has been difficult to characterize the relativistic electron population, which is determined by diffusion processes within the magnetosphere and by any local source and loss processes. Both synchrotron emission and scattering in the atmosphere contribute to the losses. Knowledge of these various processes is important to a full understanding of the Jovian magnetosphere. Spacecraft entering the Jovian magnetosphere are subjected to radiation damage from the relativistic electrons and protons providing

additional motivation to understand the processes responsible for the formation of the Jovian radiation belts.

By comparing results from a computation model of the synchrotron radiation and a realistic magnetic field model with ground based radio observations, we intend to improve the current knowledge of the relativistic electron population in the inner Jovian magnetosphere. Such modeling may also provide new information on high order moments of the field. In this paper, we outline our approach for the development of the computation model and give some initial results.

Figure 1 shows a map of Jovian synchrotron emission based on VLA observations from May 1997, at a Central Meridional Longitude (CML) of 0˚. Figure 2 shows a "beaming curve" (total power vs time for a single Jovian rotation) from single-dish data taken approximately simultaneously.

The dominant characteristics of Jovian synchrotron emission have been reviewed elsewhere [e.g. *Carr* et al. 1983]; here we note a few of the more significant characteristics:

• The bulk of the emission comes from a region roughly 3 Jovian diameters wide, near the magnetic equator, suggesting a pronounced pancake-like pitch angle distribution for the emitting relativistic electrons.

• A less intense but significant fraction of the emission comes from high-latitude lobes near 40 degrees latitude at a Jovicentric distance of about 1.4 Jovian radii, and is caused by electrons which mirror at high magnetic latitude.

• In addition to long term (months to years) variation, the total emission varies roughly sinusoidally as Jupiter rotates, peaking twice each rotation.

• Summing over the entire map, the linear polarization is about 20 to 25% and the circular polarization is roughly 2%.

In this paper we describe a computer model which calculates the synchrotron emission produced by a distribution of electrons trapped in a Jovian magnetic field. With a simple, longitudinally symmetric electron distribution, the model reproduces the gross features of the observed emission. By comparing model results with data collected from single-dish and interferometric observations, we have already begun to make inferences about Jupiter's magnetic field and the particles trapped within it.

The Model

Our model calculates the synchrotron emission map produced by a set of particles in the Jovian magnetic field, as observed from a particular direction. In contrast to earlier models [e.g. *Dulk* et al. 1999, *De Pater* 1981], our model includes a true volume integral in 3-dimensional space which takes into account the relativistic beaming effects of synchrotron emission. Synchrotron emission is highly beamed in the

instantaneous direction of motion, so the radiation from a spiralling electron is visible only as a brief pulse when its velocity vector is momentarily pointed towards the observer. To calculate the emission from a distribution of electrons, we sum up the pulses from all electrons whose pitch angle allows the velocity vector to align with the observer. Defining $\rho(E,\alpha)$ as the number of electrons per unit volume per unit energy per unit pitch angle at energy E and pitch angle α, the observed synchrotron emission can be described by its Stokes parameters [*Chang* 1962, *Legg and Westfold* 1968] as

$$I(f) = (C\,B \,/\, R^2) \int \rho(E,\alpha)\, F(f/f_c)\, dE \qquad (1)$$

$$Q(f) = -(C\,B\cos(2\chi) \,/\, R^2) \int \rho(E,\alpha)\, F_p(f/f_c)\, dE \qquad (2)$$

$$U(f) = -(C\,B\sin(2\chi) \,/\, R^2) \int \rho(E,\alpha)\, F_p(f/f_c)\, dE \qquad (3)$$

and
$$V(f) = (C\,B/R^2) \int \rho(E,\alpha)\, (4/3) i (2f/(f_B \sin\theta))^{-1/2} \cot\theta \times \{(f/f_c)^{1/2} F_s(f/f_c) + [1 + g(\theta)](f/f_c)^{-1/2}[F_p(f/f_c) - (1/2)F(f/f_c)]\} dE \qquad (4)$$

where R is the observer's distance from Jupiter, $C = 3.73 \times 10^{-23}$ erg sec^{-1} $gauss^{-1}$, B is the local magnetic field, and E is the electron energy. α is the angle between the line of sight and the magnetic field, which is the pitch angle of observable electrons, as discussed below. Definition of the Stokes parameters Q and U requires a choice of basis vectors, here taken parallel to the Jovigraphic equator, so χ is the projected angle between the magnetic field and the Jovigraphic equator. F and F_p define the frequency dependence of synchrotron emission from a single electron [*Jackson* 1975], and are defined in terms of modified Bessel functions as

$$F(x) = x \int_x^{\infty} K_{5/3}(\eta)\, d\eta \qquad (5)$$

and

$$F_p(x) = x\, K_{2/3}(x). \qquad (6)$$

The characteristic frequency, f_c , is defined by

$$f_c = 3e/(4\pi m^3 c^4)\, B \sin(\alpha)\, E^2. \qquad (7)$$

To calculate the observed emission map, we integrate the local Stokes parameters over each line of sight at the frequency of observation.

In the formulation for I, Q, and U given by Eqs. 1 through 3 above, we have made the approximation that the opening angle of the synchrotron emission beam is small compared to the pitch-angle dependence of the electron distribution. The opening angle is inversely proportional to the energy and is approximately 1.4˚ for 20 MeV electrons. Following [*Chang* 1962], we account for the opening angle of the emission in calculating the total emission, but take the approximation that all of the radiation is emitted instantaneously at the time when the particle is moving directly towards the observer. Thus the pitch angle of all emitting particles is taken to be equal to the angle between the field and the line of sight. The circular polarization, V, is a result of the finite opening angle and the

gradient of the pitch-angle distribution, and Equation 4 is taken from [*Legg and Westfold* 1968], along with the associated nomenclature. Typical observed circular polarization is about 2%.

In our computer model, we define the field and particle distributions on a 3-dimensional grid, and calculate the observed synchrotron emission by integrating Equations 1-4. The model inputs allow a choice of magnetic field model and electron density (as a function of pitch angle, energy and L-shell). Currently, we take the electron density to be

$$n_e(\alpha,L,B,E) = n_{e,\alpha}(\alpha,L,B)\, n_{e,E}(E,B) \qquad (8)$$

where L is the L-shell, defined by

$$L = (M/B_e)^{1/3} \qquad (9)$$

with B_e defined as the minimum magnetic field strength on the local field line and the magnetic dipole moment of Jupiter taken as M = 4.218 gauss-R_J^3. We further define

$$n_{e,\alpha}(\alpha,L,B) = A_L \sin^{n1}(\alpha_{eq}) + B_L \sin^{n2}(\alpha_{eq}) \qquad (10)$$

and

$$n_{e,E}(E,B) = E_0^{\varepsilon} / (E_0 + (E/B^{1/2})^{\varepsilon+0.75}) \qquad (11)$$

where A_L, B_L, n1 and n2 are functions of L, constant within each of an arbitrary number of zones, $E = E/(1\ \text{MeV})$, and $B = B/(1\ \text{Gauss})$. E_0 and ε are set at 5000 and 2.25 for all examples described in this paper. These values of E_0 and ε were chosen to roughly match the energy distribution from [*Divine&Garrett* 1983] at L=2 (Figure 3).

The atmospheric loss cone is approximated by modifying the electron distributions to remove all particles mirroring at <1 R_J at any time during a longitudinal drift period. For purposes of this calculation, shell-splitting is ignored, with particles taken to drift on surfaces of constant L, defined as $(M/B_{eq})^{1/3}$. We have calculated drift shells more exactly by tracing particle motions adiabatically, and the shell-splitting is small compared to our 0.05 R_J resolution [*Wang*, 2000].

Taking as inputs A_L, B_L, n1 and n2 for each zone in L, the model produces as outputs a map of each of the I, Q, U, and V Stokes parameters, by numerically integrating Eqs. 1-4 at each point on a grid with spacing 0.05 R_J for the volume contained by L<4. The Stokes parameters are then integrated along the line of sight (accounting for shadowing by Jupiter) to produce maps of the Stokes parameters with resolution 0.05 R_J. Model maps are made to correspond with different viewing geometries by rotating the magnetic field array prior to the calculation. For comparison with VLA data, maps from a range of CMLs are averaged together (to account for time-averaging in the VLA data) and then smoothed with a 2-dimensional Gaussian beam whose size and shape are chosen to imitate the VLA resolution. For comparison with single-

dish data, rotational averaging is not necessary, and the entire map is summed to produce a single total at each CML observed.

Discussion

The parameters $A_L(L)$, $B_L(L)$, $n1(L)$ and $n2(L)$ are chosen by comparing the resulting maps with observations. The parameters in Table 1 produce maps which qualitatively fit the observed VLA maps and beaming curves. The L-shell zones were chosen *a priori* to have physically plausible boundaries, and the parameters in each zone were then adjusted to produce reasonable maps. This was done iteratively, starting with an initial guess and successively modifying each of the $A_L(L)$ and $B_L(L)$ coefficients in an attempt to match the CML=0° VLA image. $n2(L)$ was then adjusted (keeping $n1(L)$ fixed at 1.0) to better match the East-West asymmetry, and the process was repeated, with additional small adjustments to improve the beaming curve and the match at other CML's. We have produced qualitatively similar fits to the data by using parameters which differ by ~10% from those in Table 1, and also by using the O6 [*Connerney* 1993] instead of the VIP4 [*Connerney* et al. 1998] magnetic field model. We have not fully explored variations of the energy distribution, but it is clear that a different energy distribution would require changes in the $A_L(L)$ and $B_L(L)$ coefficients.

Figure 4 shows modelled Stokes I emission at two different CML's, with the corresponding VLA images. The data were averaged over ±20° CML to improve the signal to noise ratio, so the same was done to the model maps. The model maps have also been smoothed with a Gaussian to approximate the effective elliptical shape of the VLA beam. Representative fieldlines are shown (projected onto the plane of the image) for L-shells of 1.5, 2.0, 2.5, 3.0, and 3.5 based on the VIP4 model.

Figure 5 shows model beaming curves compared to single dish data at the same value of D_E, where the model Stokes I maps have been calculated at the appropriate frequency and totalled to produce a single total-power value at each CML. The model beaming curves look similar to the actual data, with no need for longitudinal asymmetry in the particle distributions. Similarly, Figure 6 shows that the East-West asymmetry in the equatorial lobes can be matched reasonably well to the data using longitudinally symmetric electron distributions. This result contradicts previous suggestions that a "hot spot" in Jupiter's radiation belts is needed to explain the asymmetry of the synchrotron emission [e.g. *De Pater* 1991]. By changing the pitch angle distribution of the equatorial particles, one can adjust the variation in the beaming curve and the East-West asymmetry in the equatorial lobes, so the parameters chosen (Table 1) reflect an attempt to fit the model to the May 1997 data. In May 1997 the Earth was in the Jovigraphic equatorial plane (D_E = 0, top panel in Figure 5), but the same model parameters have also been used

to simulate the emission that would be observed at other viewing angles, as shown in the lower panels of Figure 5.

The parameters in Table 1 were not adjusted to fit the polarization, but there is nonetheless rough agreement between the modelled polarization and the observational data, with average total linear polarization of 26% for the model and average circular polarization of 5%.

Future Work

We plan improvements to the model in a number of areas:

• In a non-dipole field, electrons with differing pitch angles do not drift longitudinally on a single shell, and we will include a more exact definition of the electron drift.

• Electrons change pitch angle and lose energy as they produce synchrotron radiation. In the current model, this is taken into account only by the fact that the particle distributions are adjusted to fit the observed maps. We will modify the model to explicitly account for radiative losses.

• Meaningful quantitative comparison of the model maps to the observed maps is a non-trivial problem, and we are developing more quantitative figures of merit to replace the subjective comparisons done here.

• We are working with collaborators to replace *ad hoc* particle distributions like that described in Table 1 with distributions derived more explicitly from first principles.

Acknowledgements

We appreciate the advice and assistance of Dr. Robert Sault and Dr. Kaiti Wang. This research was carried out at the Jet Propulsion Laboratory, California Institute of Technology, under a contract with the National Aeronautics and Space Administration.

Figures

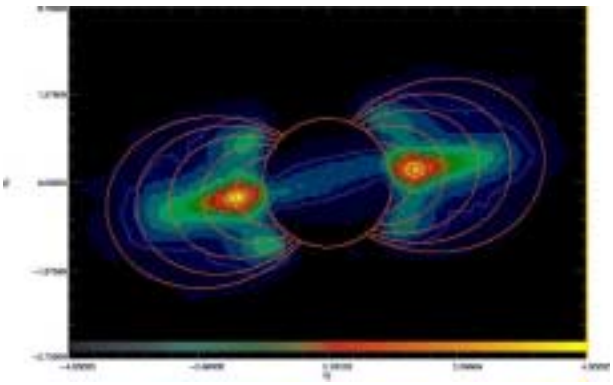

Figure 1. Map of Jovian synchrotron emission as seen at CML=120˚ in May, 1997. Representative field lines are shown in the meridional plane for L-shells of 1.5, 2.0, 2.5, 3.0, and 3.5. Thermal emission from Jupiter has been subtracted. The color scale (shown at the bottom) is linear.

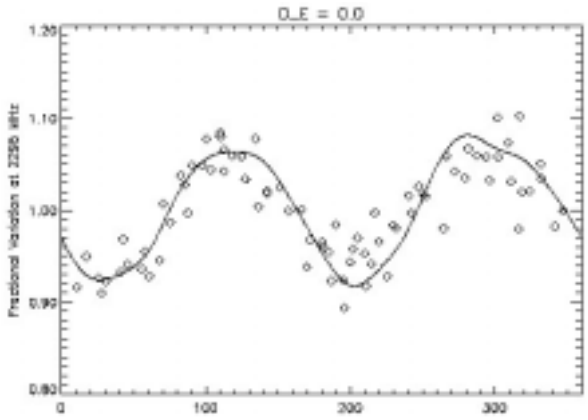

Figure 2. Example "beaming curve" (total power vs time) for Jovian emission from DSN single-dish data taken at 2295 MHz at approximately the same time as Figure 1. The solid line represents the 2295 MHz beaming curve predicted by our model with the parameter choices shown in Table 1.

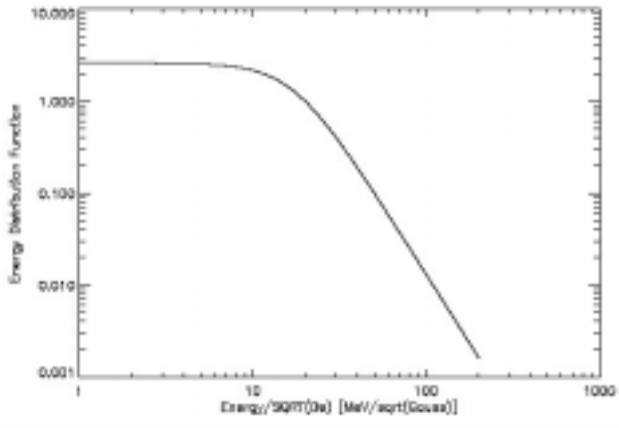

Figure 3. The energy distribution used for the examples shown in this paper.

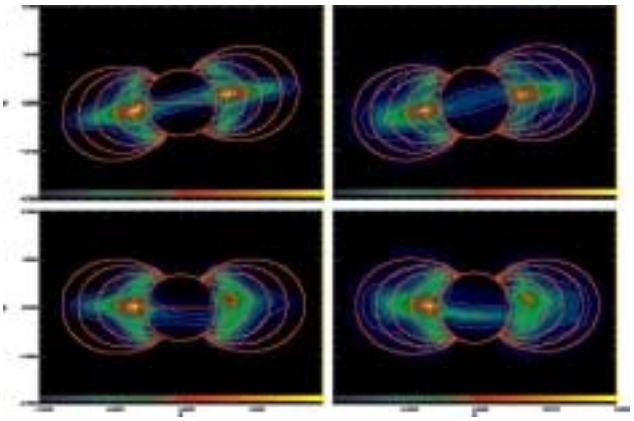

Figure 4. Comparison between VLA maps and our model (using parameters in Table 1) at 1400 MHz. The images represent model (left) and VLA (right) data for CML=120˚ (top) and 200˚ (bottom). Representative field lines are taken from the VIP4 model. Thermal emission from Jupiter has been subtracted. For each map, the color scale (shown at the bottom) is linearly normalized to the brightest pixel. Model maps are smoothed and averaged to approximate the spatial and temporal (longitudinal) resolution of the VLA observations.

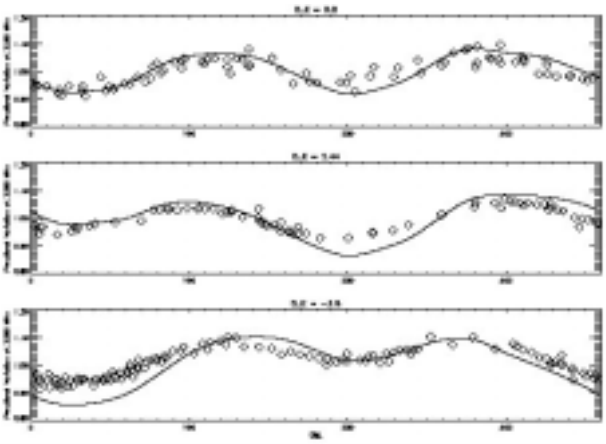

Figure 5. Observed and model beaming curves at 2295 MHz. Data were taken in 1997 (top panel), 1998 (middle panel), and 1994 (bottom panel), at times corresponding to different values of D_E , the Jovigraphic latitude of the sub-Earth point. The solid lines are model predictions (using the parameters in Table 1) for the corresponding D_E values of 0.0˚, 2.44˚, and -3.8˚.

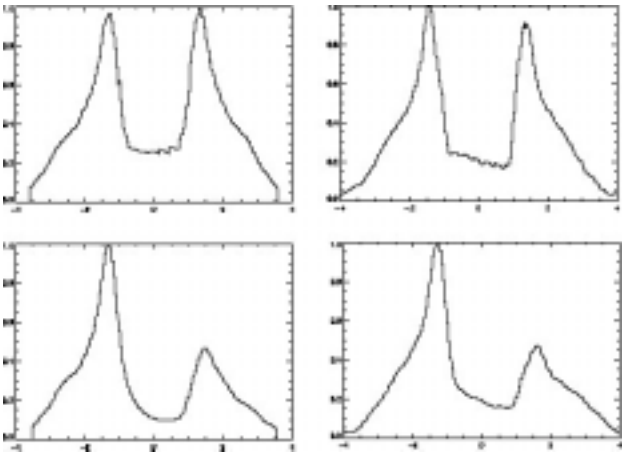

Figure 6. Comparison between model (left) and VLA observations (right) for a straight line cut along the magnetic equator. CML's of 120˚ (top) and 200˚ (bottom) are shown. In each panel, the plot is generated by extracting from the appropriate map (Figure 4) the brightness values along a straight line drawn through the magnetic equator (*i.e.*, through the Jovigraphic equator for CML = 200˚ and at an angle of 9.85˚ for CML = 120˚) and then normalizing to the peak brightness.

L-Shell	**n1**	**n2**	**A_L**	**B_L**
1.36-1.44	1.0	50.	6.0	28
1.44-1.78	1.0	46.	8.5	14.5

1.78-2.00	1.0	40.	22	10.4
2.00-2.24	1.0	40.	44	25.5
2.24-2.48	1.0	40.	45	35.7
2.48-2.80	1.0	40.	90	130
2.80-3.30	1.0	40.	125	450
3.30-3.90	1.0	40.	120	1160

Table 1. Example of a parameter set (see Eq. 10) for which the model roughly fits the data. As described in the text, these model parameters were chosen for each of 8 zones in L to match the resulting model images to VLA data taken in May of 1997. These parameter choices are used for all of the model results shown in this paper. Other parameter choices can result in similar qualitative agreement between model and data.

References

Carr, T. D., M. D. Desch, and J. K. Alexander, *Physics of the Jovian Magnetosphere*, ed. A. J. Dessler, Cambridge University Press, 1983.
Chang, D.B., and Davis, L., Jr., "Synchrotron Radiation as the Source of Jupiter's Polarized Decimeter Radiation", *ApJ* **126**, 567, 1962.
Connerney, J.E.P., "Magnetic Fields of the Outer Planets", *J. Geophys. Res*. **98**, 18659-18679, 1993.
Connerney, J.E.P. *et al.*, "New models of Jupiter's magnetic field constrained by the Io flux tube footprint.", *J. Geophys. Res*. **103**, 11929-11939, 1998.
De Pater, I., "A Comparison of Radio Data and Model Calculations of Jupiter's Synchrotron Radiation", *J. Geophys. Res*., **86**, 3397-3422, 1981.
De Pater, I., "Radio Images of Jupiter's Synchrotron Radiation at 6, 20, and 90 cm", *J. Geophys. Res*., **102**, 794-805, 1991.
DePater, I., Schultz, M., and Brecht, S., "Synchrotron evidence for Amalthea's influence on Jupiter's electron radiation belt", *J. Geophys. Res*. **102**, 22043-22064, 1997.
Divine N., and H. B. Garrett, "Charged particle distribution in Jupiter's magnetosphere":, *J. Geophys. Res.*, **88**, 6889-6903, 1983.
Dulk, G. A., et al. *A&A*, **347**, 1029-1038, 1999.
Jackson, J. D., *Classical Electrodynamics*, 2nd ed., John Wiley and Sons, 1975.
Leblanc, Y., Sault, R., and Dulk, G., "Synthesis of magnetospheric radio emissions during and after the Jupiter/SL-9 collision", *Planet. Space Sci.*, **45,** No.10, p.1213, 1997.
Legg, M.P.C., and Westfold, K.C., "Elliptic Polarization of Synchrotron Radiation", *ApJ* **154**, 499, 1968.
Wang. K., 2000, *private communication*.